A Numerical Approach to Non-Equilibrium Quantum Thermodynamics: Non-Perturbative Treatment of the Driven Resonant Level Model based on the Driven Liouville von-Neumann Formalism Supporting Information

Annabelle Oz,[1,2] Oded Hod,[1,2] and Abraham Nitzan[1,2,3]

[1] *Department of Physical Chemistry, School of Chemistry, The Raymond and Beverly Sackler Faulty of Exact Sciences, Tel Aviv University, Tel Aviv, IL 6997801*

[2] *The Sackler Center for Computational Molecular and Materials Science, Tel Aviv University, Tel Aviv, IL 6997801*

[3] *Department of Chemistry, University of Pennsylvania, Philadelphia, PA, USA 19103*

The following items appear in this supporting information:

1. DLvN driving rate (Γ) Sensitivity Check.
2. Finite Bandwidth Lead Model Sensitivity Check.
3. Lead Density of States Sensitivity Check.
4. Evaluation of the Lead Contribution to Quasi-Static Observable Variations.

1. DLvN Driving Rate (Γ) Sensitivity Check

The results presented in the main text were obtained using a finite lead model of $N_L = 100$ levels and a bandwidth of 10 (in units of $\hbar\gamma$). Correspondingly, the DLvN driving rate was set to broaden the lead levels according to their spacing such that $\hbar\Gamma = \Delta\varepsilon = 0.1$. To verify that our results are sufficiently insensitive to this driving rate choice we repeated the excess dot occupation and energy contribution calculations using $\dot{\varepsilon}_d = 0.1$ (in units of $\hbar\gamma^2$) for a lead model size of $N_L = 200$, of bandwidth 10, electronic thermal energy of $K_BT = 0.5$, dot level shift rate of $\dot{\varepsilon}_d = 0.1$, and three values of the DLvN driving rate: $\Gamma = \Delta\varepsilon = 0.05$, $\Gamma = 2\Delta\varepsilon = 0.10$, and $\Gamma = 3\Delta\varepsilon = 0.15$. The results presented in Figs. S1-S2 demonstrate that our numerical calculations are insensitive to the choice of Γ within the range of values considered.

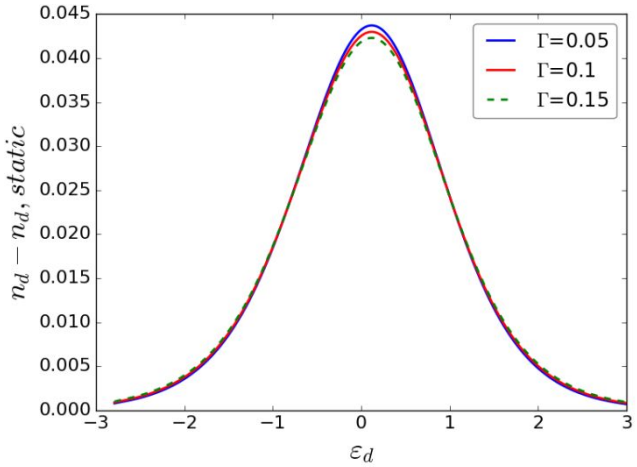

Figure S1: Excess dot occupation as a function of ε_d for a DLvN driving rate of $\Gamma = 0.05$ (Full blue line), $\Gamma = 0.10$ (Full red line) and $\Gamma = 0.15$ (Dashed green line). In all calculations $\dot{\varepsilon}_d = 0.1$, $K_BT = 0.5$, the lead bandwidth is 10, and the lead size is $N_L = 200$.

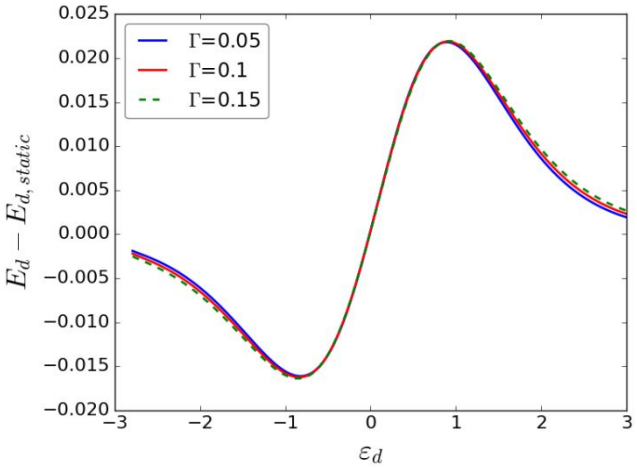

Figure 1S2: Excess dot energy contribution as a function of ε_d for a DLvN driving rate of $\Gamma = 0.05$ (Full blue line), $\Gamma = 0.10$ (Full red line) and $\Gamma = 0.15$ (Dashed green line). In all calculations $\dot{\varepsilon}_d = 0.1$, $K_BT = 0.5$, the lead bandwidth is 10, and the

lead size is $N_L = 200$.

2. Finite Bandwidth Lead Model Sensitivity Check

The results presented in the main text were obtained using a finite lead model size of 100 levels spanning a bandwidth $10\,\hbar\gamma$. To verify that our results are sufficiently insensitive to this bandwidth choice we repeated the quasi-static dot occupation, entropy, and heat calculations using a lead bandwidth of $20\hbar\gamma$. To keep the density of lead states constant we also doubled the number of finite lead model levels to 200. The rest of the parameters were the same as those used for the calculations presented in the main text ($\gamma = 1$, $\Gamma = \Delta\varepsilon = 0.1$, and $k_BT = 0.5$). The results presented in Figs. S3-S5 demonstrate that our numerical calculations, which (as discussed in the main text) are in good agreement with the analytical WBL results, are fairly insensitive to the choice of lead bandwidth. Furthermore, the minor changes associated with doubling the bandwidth of the finite lead model make the agreement between the numerical calculation and the WBL expression even better. Therefore, we may conclude that our numerical results using the finite lead model are converged to the WBL case. We note again that our numerical calculations are not limited to the wide-band approximation and the choice to approach this limit here is made deliberately for the purpose of comparison with the analytical expressions.

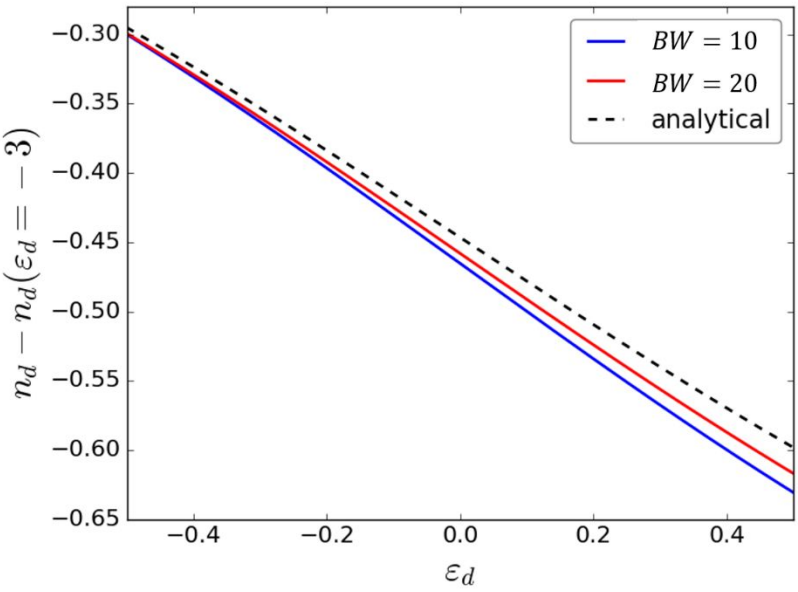

Figure S3: Quasi-static dot occupation measured relative to its values at $\varepsilon_{d1} = -3$, plotted against the dot energy ε_d for lead model bandwidth of $10\hbar\gamma$ (full blue line) and $20\hbar\gamma$ (full red line) compared to the analytical WBL results (dashed black line). The full blue line and the dashed black line are the same as those appearing in Fig. 2a of the main text.

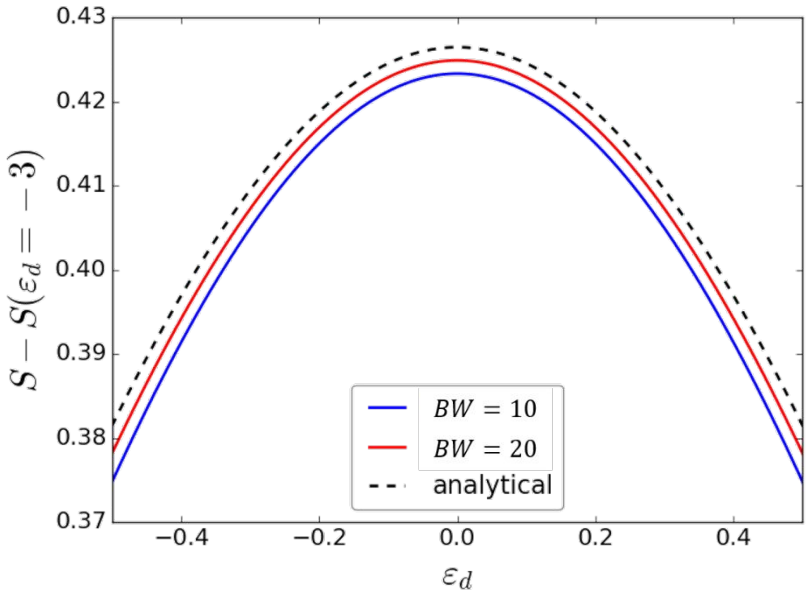

Figure S4 Entropy (calculate via Eq. (22) of the main text) measured relative to its value at $\varepsilon_{d1} = -3$, plotted against the dot energy ε_d for lead model bandwidth of $10\hbar\gamma$ (full blue line) and $20\hbar\gamma$ (full red line) compared to the analytical WBL results (dashed black line). The full blue line and the dashed black line are the same as those appearing in Fig. 2c of the main text.

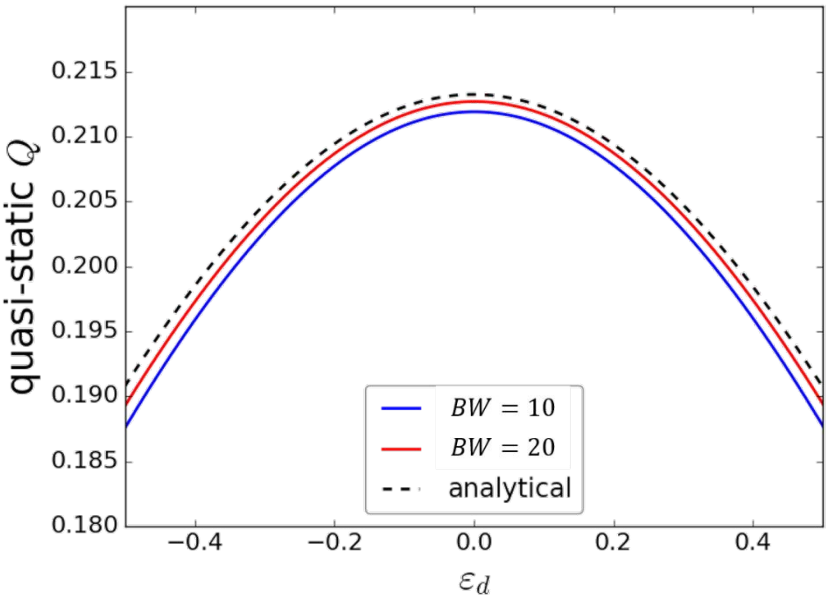

Figure S5: Heat measured relative to its value at $\varepsilon_{d1} = -3$, plotted against the dot energy ε_d for lead model bandwidth of $10\hbar\gamma$ (full blue line) and $20\hbar\gamma$ (full red line) compared to the analytical WBL results (dashed black line). The full blue line and the dashed black line are the same as those appearing in Fig. 3b of the main text.

3. Lead Density of States Sensitivity Check

The results presented in the main text were obtained using a finite lead model of $N_L = 100$ levels and a bandwidth of 10 (in units of $\hbar\gamma$). yielding a lead inter level spacing of $\Delta\varepsilon = 0.1$ (in units of $\hbar\gamma$). To verify that our results are converged with respect to the density of lead states we repeated the excess dot occupation and energy contribution calculations using $\dot{\varepsilon}_d = 0.1$ (in units $\hbar\gamma^2$) for a lead model size of $N_L = 200$ at the same lead bandwidth yielding a lead inter level spacing of $\Delta\varepsilon = 0.05$. The calculations were performed at a dot level shift rate of $\dot{\varepsilon}_d = 0.1$ and bath electronic thermal energy of $K_BT = 0.5$. The DLvN driving rate was set to broaden the lead levels according to their spacing such that $\hbar\Gamma = \Delta\varepsilon$. The results presented in Figs. S6-S7 demonstrate that our numerical calculations, are well converged with respect to the density of finite lead model states.

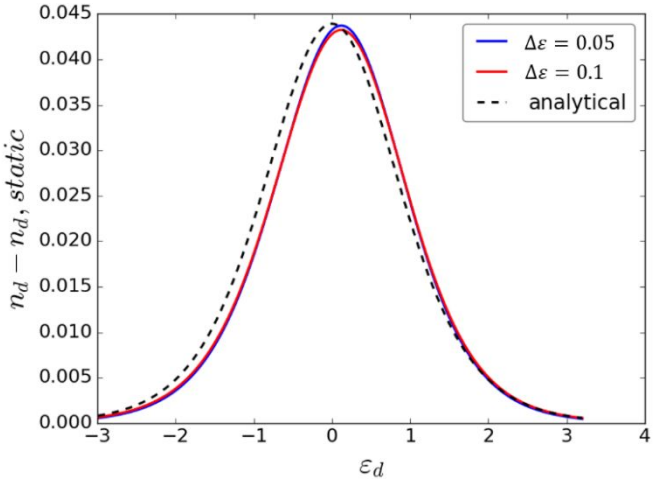

Figure S6: Excess dot occupation as a function of ε_d for lead inter-level spacing of $\Delta\varepsilon = 0.1$ (full red line) and $\Delta\varepsilon = 0.05$ (full blue line). In both cases we take $\dot{\varepsilon}_d = 0.1$, $K_BT = 0.5$, lead bandwidth of 10, and $\Gamma = \Delta\varepsilon$.

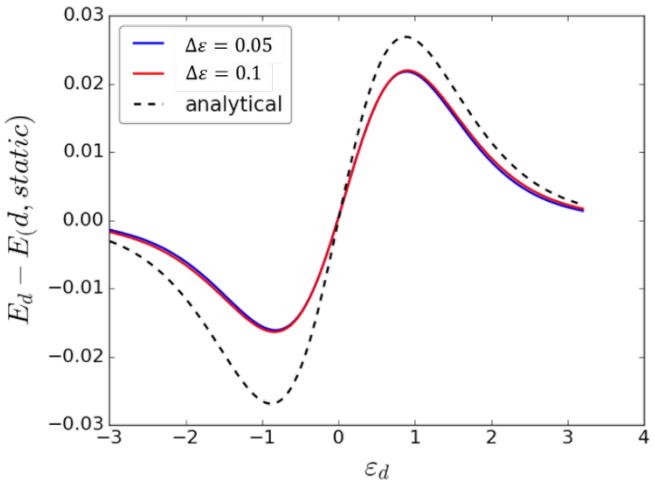

Figure S7: Excess dot energy contribution as a function of ε_d for lead inter-level spacing of $\Delta\varepsilon = 0.1$ (full red line) and $\Delta\varepsilon = 0.05$ (full blue line). In both cases we take $\dot{\varepsilon}_d = 0.1$, $K_BT = 0.5$, lead bandwidth of 10, and $\Gamma = \Delta\varepsilon$.

4. Evaluation of the Lead Contribution to Quasi-Static Observable Variations

In the main text, when comparing the results of our numerical calculations to the WBL analytical expressions, we have focused on the dot's contribution to the variations in particle number and energy. Indeed, in the analytical treatment the lead (representing the entire bath) is assumed to be constantly at equilibrium regardless of the dot dynamics. Hence, all variations occur at the dot itself and its interface with the lead. On the contrary, in our numerical treatment the coupled dot-lead dynamics is considered explicitly. Since the lead is driven towards equilibrium at a finite rate, its dynamical state in any given instance only approximates the desired equilibrium.

To test how much this influences the comparison with the WBL analytical results we have repeated the equilibrium numerical calculations comparing the variations in the number of particles and energy of the entire dot-lead system compared to the dot contributions alone. To this end, we assigned Fermi-Dirac occupations to the eigenstates of the Hamiltonian of the dot-lead system at different dot level positions and compared the variations in the total number of electrons and energy to their projection on the dot site. The small deviations reflected in Figs. S8 and S9 indicate that the lead's deviation from equilibrium, at least under quasi-static conditions, is minor and that most of the variations occur at the dot. Nevertheless, the total dot-lead observables provide a somewhat better fit to the WBL analytical results than the dot contribution alone.

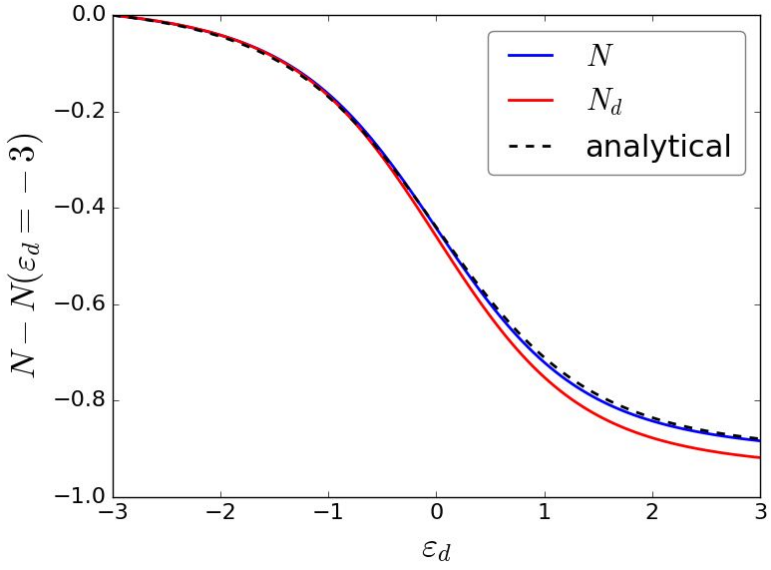

Figure S8: Equilibrium dot (full blue line) and dot-lead (full red line) occupations measured relative to their values at $\varepsilon_{d1} = -3$, plotted against the dot energy ε_d. Results obtained via the analytical WBL expression are presented by the dashed-black line. The results were obtained at an electronic temperature corresponding to $K_B T = 0.5$ (in units of $\hbar\gamma$) using a finite lead model of $N_L = 100$ levels and a bandwidth of 10. Correspondingly, the DLvN driving rate was set to broaden the lead levels according to their spacing such that $\Gamma = \Delta\varepsilon = 0.1$.

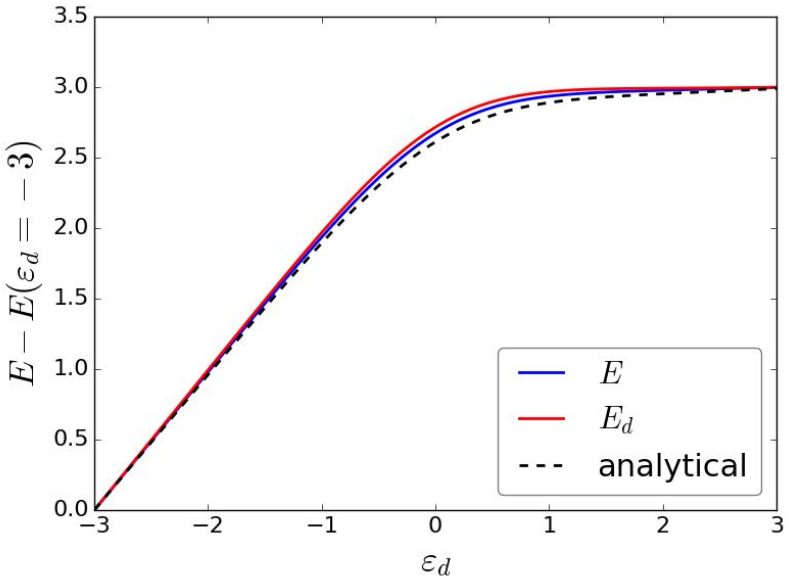

Figure S9: Equilibrium dot (full blue line) and dot-lead (full red line) energies measured relative to their values at $\varepsilon_{d1} = -3$, plotted against the dot energy ε_d. Results obtained via the analytical WBL expression are presented by the dashed-black line. The results were obtained at an electronic temperature corresponding to $K_B T = 0.5$ (in units of $\hbar\gamma$) using a finite lead model of $N_L = 100$ levels and a bandwidth of 10. Correspondingly, the DLvN driving rate was set to broaden the lead levels according to their spacing such that $\Gamma = \Delta\varepsilon = 0.1$.